Ab initio study of lithium intercalation in metal oxides and metal dichalcogenides

M. K. Aydinol, A. F. Kohan, and G. Ceder
Department of Materials Science and Engineering, Massachusetts Institute of Technology, Cambridge, Massachusetts 02139

K. Cho and J. Joannopoulos
Department of Physics, Massachusetts Institute of Technology, Cambridge, Massachusetts 02139

(Received 31 January 1997)

A study of the average voltage to intercalate lithium in various metal oxides is presented. By combining the *ab initio* pseudopotential method with basic thermodynamics the average intercalation voltage can be predicted without the need for experimental data. This procedure is used to systematically study the effect of metal chemistry, anion chemistry, and structure. It is found that Li is fully ionized in the intercalated compounds with its charge transferred to the anion and to the metal. The substantial charge transfer to the anion is responsible for the large voltage difference between oxides, sulfides, and selenides. Ionic relaxation, as a result of Li intercalation, causes nonrigid-band effects in the density of states of these materials. Suggestions for compounds that may have a substantially larger voltage than currently used materials are also presented. [S0163-1829(97)01028-X]

I. INTRODUCTION

Considerable interest exists in lithium-metal-oxides due to their application potential as rechargeable battery electrodes[1] and electrochromic displays.[2] These oxides derive their interesting properties from the large stability region they have with respect to lithium content. In some materials, the ratio of lithium to metal ions can be varied between 0 and 1 without substantial changes to the structure of the material. This topotactic Li-intercalation mechanism is the basis for the material's application as an electrode in a rechargeable battery. When used as a cathodic electrode for example, Li is accumulated in the oxide structure during the discharge cycle of the battery, and is removed again upon charging. It is believed that Li is fully ionized in most lithium-metal oxides and donates its electron to the host bands without much affecting them. This makes it possible to control the band filling of the host material by varying the Li content electrochemically. In electrochromic applications, band filling is used to adjust the electronic and optical properties.[3]

Figure 1 shows schematically an electrochemical lithium cell. Two electrodes, the anode and cathode, are separated by an electrolyte. The electrolyte allows transfer of Li ions between the anode and cathode but does not allow for any electron transport. In most applications the electrolyte is liquid, although glasses[4] and solid polymers[5] are being investigated as more versatile alternatives. The equilibrium voltage difference between the two electrodes, also referred to as the open circuit voltage (OCV), depends on the difference of the Li chemical potential between the anode and cathode

$$V(x) = -\frac{\mu_{\mathrm{Li}}^{\mathrm{cathode}}(x) - \mu_{\mathrm{Li}}^{\mathrm{anode}}}{zF}. \qquad (1)$$

F is the Faraday constant and z is the charge (in electrons) transported by lithium in the electrolyte. In most nonelectronically conducting electrolytes $z=1$ for Li intercalation. For a battery, a large chemical-potential difference between cathode and anode is desirable as this leads to a high OCV. For electrochromic applications the voltage is less important. In this paper we will assume an anode of metallic lithium, although for practical applications, lithium-carbon solutions are preferred.[6] Our results can be easily modified for other anodes as the choice of anode only changes the reference chemical potential used in Eq. (1). $LiCoO_2$ is one of the materials currently used as an active cathode material in commercial batteries[7,8] and has an OCV of about 4 V with respect to metallic lithium. Such high cell voltage, typical for transition-metal oxides, combined with a relatively high charge-storage capacity, highlights the potential of these materials in high-energy-density rechargeable batteries.

Metal-oxide electrodes have to meet several design criteria.[9–11] A high intercalation voltage and low molar weight are desirable from the standpoint of obtaining an electrode with high-energy density. The composition range over which Li can be reversibly intercalated determines the battery capacity. For low Li content, many of the lithium-transition-metal oxides undergo irreversible structural changes, thereby destroying part of the capacity that can be

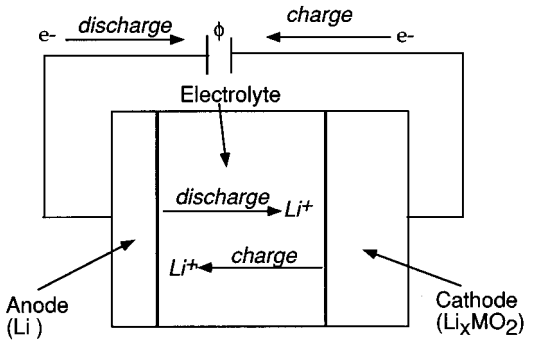

FIG. 1. Schematic picture of a rechargeable electrochemical Li cell. When the battery discharges Li is intercalated into the cathode compound. Upon charging the Li ions are removed from the cathode.

used in the next discharge cycle. High Li diffusivity is important to satisfy the current-density requirements. Although Li diffusivities reported in the literature are often conflicting, diffusion coefficients as high as 10^{-7} cm^2/s at room temperature have been measured for Li^+ in $LiNiO_2$.[12] Some electronic conductivity in the material is necessary to transport the electrons that compensate for the intercalation of Li^+ ions.

The band structure of intercalation compounds has been studied extensively with electronic structure methods. Since the host material is typically little affected structurally by the intercalation of lithium, and lithium is fully ionized to Li^+, it has been argued[13] that the effect of Li intercalation is to increase the filling of the bands of the host material. In this rigid-band picture, Li intercalation causes the Fermi level to rise, and the intercalation curve $V(x_{Li})$, the variation of the voltage with the Li content of the cathode, therefore reflects the shape of the density of states at the Fermi level. This rigid-band model has been modified to account for the electrostatic effect of the Li^+ ion on the band structure of the host material[14–16] since the positive field from Li^+ lowers the electronic states of the host. In this modified rigid-band model, the Fermi level remains unchanged as Li is intercalated, but the density of states translates to lower energies. Using a semiempirical tight-binding Hamiltonian McCanny[17] computed the band structure of $LiTiS_2$ and TiS_2 at the experimentally determined lattice parameters and found that the bands derived from the metal or chalcogenide *s* orbitals shifted considerably upon intercalation of lithium. Most of McCanny's observations were later confirmed with more accurate linear augmented plane-wave (LAPW) calculations.[18] Linear muffin-tin orbital in the atomic-sphere approximation (LMTO-ASA) results on TaS_2 and $LiTiS_2$ also indicated changes in the band structure as a result of intercalation.[19] The rigid-band model has also been questioned from the experimental side.[14]

Attempts to obtain intercalation voltages with first-principles calculations are limited and have focused solely on the band structure of the material.[13,20] Miura tried to deduce intercalation voltages from the calculated energy levels in clusters of lithium-manganese-oxide.[20] The energy levels of the clusters were computed with the discrete variational X-α method. Although this approach may lead to some insight in the relation between band structure and intercalation voltage it cannot be used for quantitative predictions due to the lack of an absolute energy scale and the arbitrariness of the structural relaxation imposed by the cluster boundary condition. It is doubtful that the electronic density of states can be related to the intercalation voltage in a quantitative matter as is often inferred.[13,20,21] As argued by McKinnon[22] the separation of the intercalation energy into an electronic part and an ionic part is arbitrary, due to the strong interaction between the Li ion and the electron it has donated to the host material. A true intercalation energy can only be obtained from the total-energy chemical potential of lithium.

In this paper we present first-principles pseudopotential calculations to study the intercalation properties of various lithium-metal-oxides, sulfides, and selenides. We focus on the intercalation voltage and demonstrate how it can be accurately predicted by means of first-principles techniques. In our approach there is no need to separate the intercalation energy into an electronic and ionic part since we will obtain predicted voltages from the total energy of the intercalated and deintercalated compounds. To calculate the total energies we use the pseudopotential method. In Secs. III and IV we show that this procedure gives good agreement with available experimental data. Since we need no experimental input to the calculations, it is possible to calculate the intercalation voltage for nonexisting chemistries and structures. This allows us to systematically investigate the effect of structure, metal chemistry, and anion chemistry on the intercalation voltage. In Sec. III we demonstrate that all three are responsible for substantial variations in the voltage, although the role of structure is found to be indirect, through the symmetry constraints placed on the ionic relaxations. One remarkable result we find is a very large effect from the anion on the intercalation voltage. By studying the variations in charge density upon intercalation we will show that this is due to the large charge electron transfer from Li to the anions. This is contradictory to the common belief that most of the charge transfer is with the transition-metal ion. Comparison between the band structures of the intercalated and deintercalated materials indicates a considerable amount of nonrigid-band behavior. Finally, we suggest compounds which may have a considerably larger intercalation voltage than currently used materials.

II. THE PSEUDOPOTENTIAL METHOD

Although several first-principles methods can be used to calculate the electronic structure of metal oxides, most are not accurate enough to provide reliable values of the optimized geometries and cohesive energies.[23] Methods using spherical approximations, such as the LMTO-ASA method, previously applied to a study of $(Li)TiS_2$,[19] suffer from an arbitrariness in determining the atomic sphere sizes. By comparatively testing different methods[23] we have found that only methods in which no shape approximation to the electronic potential is made can reliably predict crystal parameters and reaction energies in oxides.

Many of the modern quantum-mechanical techniques to compute total energies are based on the density-functional theory.[24] This framework allows, in principle, to exactly map the problem of solving the Schrödinger equation for many interacting electrons onto that of a single electron moving in a nonlocal potential. This potential is not known exactly and several approximations are used to represent it. One of the most used expressions is a local representation of the effective potential called the local-density approximation (LDA).[25] We will solve the Schrödinger equation within the LDA by using the pseudopotential method. Although originally developed for metals and semiconductors, the accuracy of the pseudopotential technique for oxides is now well established.[23,26–30] In previous work we found that crystallographic parameters and energies of mixing could be well predicted with the pseudopotential method.[23,31]

In the pseudopotential method the core electrons are assumed to remain unchanged when forming the solid (frozen-core approximation), so that only the valence electrons need to be considered in the Schrödinger equation. The effect of the core electrons on the valence states is taken into account by the *pseudopotential*. This replaces the strong electron-ion

TABLE I. Core radii, in a.u., used in the generation of the pseudopotentials.

	Li	O	Al	S	Ti	V	Mn	Co	Ni	Cu	Zn	Se
r_s	2.2	0.8	2.0	1.8	2.54	2.54	2.0	1.9	2.1	2.0	2.3	1.9
r_p	2.2	0.8	2.0	1.8	2.96	2.96	2.13	2.0	2.2	2.29	2.5	1.9
r_d					1.95	1.95	1.96	2.0	2.0	1.88	1.83	1.9

potential with a much weaker pseudopotential allowing the use of planes waves for the expansion of the valence wave functions. The pseudopotential is constructed so that the valence wave functions have no radial nodes inside the core. In this way, we are effectively replacing the valence electronic wave functions by pseudo wave functions. Since most physical properties depend on the behavior of the valence electrons outside the core, the pseudopotential approximation is usually a very accurate one. In this work we use nonlocal norm-conserving pseudopotentials in the Kleinman-Bylander form.[32] For all elements, the *s* component is taken as the local pseudopotential component, except for Se where the *p* component is local. Details of the parameters chosen to generate the pseudopotentials are described in Table I. To accelerate the convergence of the plane-wave expansion we used optimized pseudopotentials.[33] These reduce considerably the size of the basis needed to accurately compute energies in materials with sharply peaked valence orbitals (as is the case in transition metals and oxygen). The number of basis functions is specified by a cutoff energy, beyond which plane waves with higher kinetic energies are excluded from the expansion. In all the calculation we used a 900-eV cutoff.

To benchmark the pseudopotential calculations we have also performed all-electron calculations in the full-potential linearized augmented plane-wave method (FLAPW) for $LiCoO_2$. ($R_{\rm mt}K_{\rm max}=9.5$ and 600 total k points).

III. THE INTERCALATION VOLTAGE

The open-cell voltage that can be derived from Li intercalation between a lithium anode and a lithium-metal-oxide cathode depends on the lithium chemical potential in the cathode [see Eq. (1)]. As Li is intercalated, its chemical potential in the cathode increases, leading to a decrease in the cell voltage. This *intercalation curve*, $V(x_{\rm Li})$, has been measured experimentally for several Li_xMO_2 materials. In general, a relatively flat intercalation curve is desirable for applications, although some slope to the curve is useful to relate the OCV to the level of intercalation during charge and discharge.

It is not possible to compute $V(x_{\rm Li})$ solely with total-energy methods (except for $x=0$ or 1) as the lithium ions in Li_xMO_2 may be partially disordered. The state of long- or short-range order of the lithium ions will influence the lithium chemical potential and hence the cell voltage. The methodology to compute the free energy of systems with site disorder is well known:[34–39] The dependence of the free energy on site disorder can be parametrized with a cluster expansion.[38] Usually the total energy of 10–20 configurations of the disordered ions is required to parametrize the cluster expansion correctly, including structures with considerably larger unit cells than the ones used here. Using energies calculated by Sluiter *et al.*,[40] Reimers and Dahn[41] applied this method to compute $V(x_{\rm Li})$ in $AlLi_x$ alloys. Due to the more complex crystal structure and electronic structure of the intercalation oxides, this is currently unfeasible for these materials with the pseudopotential method. Progress on faster total-energy methods, applicable to oxides, may however change this situation.[23,31] Here we instead calculate the *average intercalation* voltage. We will show that this quantity can be determined from the total energy of three structures with small unit cells.

In a metallic Li anode the chemical potential is constant and equal to the Gibbs free energy of Li metal. The electrical energy obtained by discharging between $Li_{x_1}MO_2$ and $Li_{x_2}MO_2$ ($x_2>x_1$) is the integral of the voltage times the displaced charge [$q_{\rm tot}=e(x_2-x_1)$]:

$$E=\int_0^{q_{\rm tot}}V(x)dq=-\int_0^{q_{\rm tot}}\frac{\mu_{\rm Li}^{\rm IC}(x)-\mu_{\rm Li}^0}{e}\,dq. \qquad (2)$$

In Eq. (2) $\mu_{\rm Li}^{\rm IC}(x)$ is the chemical potential of Li (per atom) in the intercalation compound, $\mu_{\rm Li}^0$ is the chemical potential in metallic Li, and e is the electronic charge. If all the displaced charge is due to Li, $dq=e\,dx$, resulting in

$$\begin{aligned}E&=-\int_{x_1}^{x_2}[\mu_{\rm Li}^{\rm IC}(x)-\mu_{\rm Li}^0]dx_{\rm Li}\\&=-[G_{{\rm Li}_{x_2}MO_2}-G_{{\rm Li}_{x_1}MO_2}-(x_2-x_1)G_{\rm Li}]\\&\equiv-\Delta G_r. \qquad (3)\end{aligned}$$

The average voltage is then

$$\overline{V}=\frac{-\Delta G_r}{(x_2-x_1)F}. \qquad (4)$$

Equation (4) allows one to compute the average voltage between any two intercalation limits. For most values of x it is difficult to compute the Gibbs free energy as the Li disorder makes the system nonperiodic. Even if one attempted to approximate these structures with a periodic system, one is faced with the task of coming up with reasonable superstructures for Li as a function of composition. Currently, very little is known about the nature of the Li ordering for compositions between $x=0$ and 1. We therefore set the intercalation limits in this study to $x=0$ and 1. This leads to structures with fairly small unit cells and no configurational Li disorder. The intercalation limits $x=0$ and 1 are not completely realistic. In many cases, the host structure Li_xMO_2 becomes unstable for x approaching zero, and intercalation cycles are done in a more limited concentration range. The *average* voltage over the theoretical cycle ($0\leqslant x\leqslant 1$) should, however, not be too different from the experimentally measured values.

The calculation of the average voltage between these intercalation limits requires three total energies: The energy of metallic lithium in the body-centered-cubic structure and the energies of $LiMO_2$ and MO_2. If Li removal from $LiMO_2$ occurs completely topotactically, the structure of MO_2 will be identical to the $LiMO_2$ structure but with the Li ions removed (and the remaining ions relaxed). In some systems, such as Li_xNiO_2 this approximation is not completely valid as Li removal leads to Ni ions migrating into sites previously occupied by lithium.[42–44] Comparison of calculated and experimental results for this system should therefore be done with care. Calculations can be significantly simplified by further approximating ΔG_r ($\equiv \Delta E_r + P\Delta V_r - T\Delta S_r$) by the change in internal energy (ΔE_r) at 0 K. We expect this approximation to be quite good since the term $P\Delta V_r$ is of the order of 10^{-5} electron volts whereas ΔE_r is of the order of 3–4 eV per molecule. The term $T\Delta S_r$ is of the order of the thermal energy which is also much smaller than ΔE_r.

Having described a method to compute the average intercalation voltage, our objective is to investigate the effect of three variables in the cathode material: the selection of the metal M, the cation ordering over octahedral sites, and the effect of substitution of the anion. To clearly identify the effect of these variables on the intercalation voltage we will vary only one variable at a time. This is an advantage ''computational experiments'' have over real experiments, as cation ordering and structure are determined by the chemistry of M and are difficult to vary independently in real experiments.

IV. RESULTS

A. Effect of the metal cation (M) in $LiMO_2$

Li intercalates into the cathode as a positive ion. It is traditionally assumed that the compensating electron reduces the metal ion. The nature of the metal (M) and the strength of its M^{IV}/M^{III} redox couple is therefore expected to be a significant variable in determining the intercalation voltage. To separate the effect of metal chemistry from that of structural changes we chose to compute the intercalation voltages for a series of compounds with eight different choices of M, but all in the same structure, even when that is not the ground-state structure for the particular material. The choices are M = Ti, V, Mn, Co, Ni, Cu, Zn, and Al. We opted for the α-$NaFeO_2$ structure, as it is the equilibrium structure for $LiCoO_2$, a well studied and commercially used cathode compound.[7,45] $LiAlO_2$ and $LiVO_2$ (Ref. 46) are also stable in this structure. $LiNiO_2$ (Refs. 47 and 48) exists in a Jahn-Teller distorted variant of α-$NaFeO_2$ and usually exhibits site disorder between the lithium and nickel ions. $LiMnO_2$,[47] $LiTiO_2$ (Refs. 47 and 49) and $LiCuO_2$ (Ref. 50) form other structures, and no experimental data is available on $LiZnO_2$.

The α-$NaFeO_2$ structure (space group $R\bar{3}m$) is shown in the hexagonal setting in Fig. 2. Although a smaller rhombohedral cell can be defined with only four ions, the hexagonal setting more clearly reflects the layered nature of the material. The cations reside in planes of octahedral sites between the hexagonally stacked close-packed oxygen layers. The Li and M ions occupy alternate planes. Upon Li removal the repulsion between the oxygen planes on each side of the Li plane increases, but the O-Co-O sandwiches contract. In $LiCoO_2$, almost all of the Li ions can be removed without significant changes in the symmetry of the structure.[51]

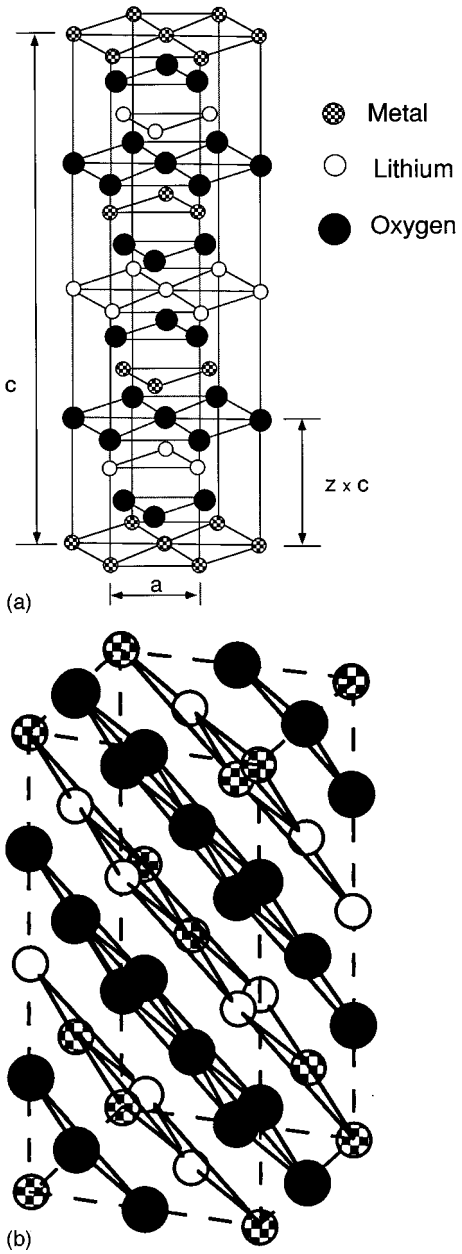

FIG. 2. (a) α-$NaFeO_2$-type structure. The oxygen ions form a cubic close-packed array and the metal cations occupy layers of octahedral interstitials. In Pearson notation the structure is $hR4$. (b) Structure of $LiScO_2$ (Pearson notation $tI16$). This structure is similar to the one in (a) but the cations are intermixed in the cation layers.

There are three variable crystal parameters in the α-$NaFeO_2$ structure: the a and c lattice parameter and an internal parameter z. [See Fig. 2(a) for the definition of z.] The energy of all MO_2 and $LiMO_2$ compounds was fully optimized with respect to these three parameters so as to obtain the minimum value of the energy consistent with the space group. Relaxations that distort (locally) the $R3m$ symmetry were not probed. Jahn-Teller distortions, such as the

TABLE II. Computed crystallographic parameters for $LiMO_2$ compounds in the α-$NaFeO_2$ structure. Experimental values are supplied in parentheses whenever available. The parameters are defined in Fig. 2(a).

	a (Å)	c (Å)	z	V (Å^3)
TiO_2	3.01	12.8	0.255	33.48
$LiTiO_2$	2.98	14.1	0.25	36.15
VO_2	2.88	12.4	0.248	29.69
$LiVO_2$	2.88	14.2[a]	0.251	34.00
	(2.84)[a]	(14.7)		(34.23)
MnO_2	2.90	12.2	0.258	29.62
$LiMnO_2$	2.92	13.5	0.256	33.23
CoO_2	2.88	12.26	0.259	29.36
$LiCoO_2$	2.93	13.2[b]	0.260	32.71
	(2.82)[b]	(14.04)	(0.264)[b]	(32.23)
NiO_2	2.87	11.72	0.255	27.87
$LiNiO_2$	2.99	12.85	0.258	33.16
	(2.88)[b]	(14.19)[b]	(0.259)[b]	(33.98)
CuO_2	2.98	11.2	0.253	28.71
$LiCuO_2$	3.05	12.7	0.256	34.10
ZnO_2	3.06	11.2	0.248	30.27
$LiZnO_2$	3.10	12.84	0.253	35.62
AlO_2	3.0	11.3	0.252	29.36
$LiAlO_2$	2.96[c]	13.35	0.257	33.76
	(2.8)	(14.23)[c]		32.21

[a]Reference 47.
[b]Reference 64.
[c]Reference 65.

one known to occur in $LiNiO_2$ are therefore not accounted for. Table II shows the calculated lattice parameters for the different compounds. Where available, experimental data is added in parenthesis. The errors in the individual lattice parameters are somewhat larger than is expected from the local-density approximation, but the overall errors in the volume are still reasonable.

The metal-oxygen bond length is shown in Fig. 3 for the lithiated and unlithiated compounds. The metal-oxygen distance decreases from Ti to Co for $LiMO_2$ and from Ti to Ni for the unlithiated MO_2 material, after which the bond length increases again.

Table III shows the average intercalation voltage obtained for the different metal oxides. For the $3d$ metals, the voltage generally increases as one goes to the right in the Periodic Table. The drop at $M=$Ni will be discussed later. $LiAlO_2$ has the highest intercalation voltage of all.

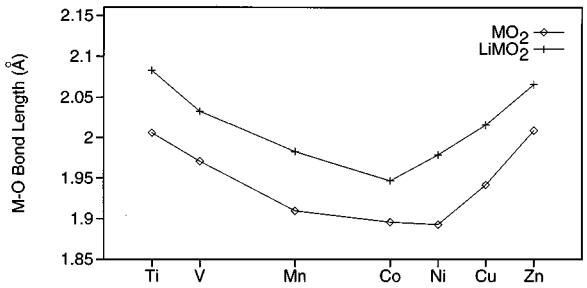

FIG. 3. Metal-oxygen distance in lithiated and unlithiated compounds as a function of d-band filling.

B. Effect of anion chemistry

A significant volume of work on alkali-metal intercalation in sulfides exists[10,22] although it is now recognized that oxides have higher intercalation voltages. This is confirmed by our results in Table IV where the intercalation voltage is presented for the reaction

$$CoX_2 + Li \rightarrow LiCoX_2, \tag{5}$$

with $X=$O, S, and Se. The heavier chalcogenides give a considerably lower voltage than the oxide. Calculations were performed in the α-$NaFeO_2$ structure so as to eliminate structural effects on the voltage. To our knowledge, neither $LiCoS_2$ or $LiCoSe_2$ have been synthesized.

C. Effect of structure and local relaxation

$LiMO_2$ compounds form in several different structures. Experimental voltage differences between cathodes with various metals may therefore be a combination of structural and chemical effects. The advantage of a computational investigation is that these effects can be well separated. In Table V the calculated intercalation voltage for $LiCoO_2$ in two different structures is shown. We chose two structures in

TABLE III. Average intercalation voltage for Li in various $LiMO_2$ compounds in the α-$NaFeO_2$ structure as calculated with the pseudopotential method.

M in $LiMO_2$	Ti	V	Mn	Co	Ni	Cu	Zn	Al
Av. voltage (V)	2.14	2.81	3.13	3.75	2.92	3.66	4.41	4.7

TABLE IV. Average intercalation voltage for Li in various $LiCoX_2$ compounds in the α-$NaFeO_2$ structure as calculated with the pseudopotential method.

X in $LiCoX_2$	O	S	Se
Av. voltage (V)	3.75	2.04	1.46

which the lithium and metal ions are octahedrally coordinated. One is the layered structure of α-$NaFeO_2$, shown in Fig. 2(a). We refer to this structure by its Pearson symbol[52] $hR4$. The second one is the $tI16$ structure shown in Fig. 2(b). It is related to $hR4$ but the Co and Li ions are now intermixed in the cation layers. This structure is found in $LiScO_2$ and sometimes in $LiFeO_2$.[47] For each structure, two intercalation voltages are given in Table V. The *relaxed* value takes into account all displacements of ions and changes in cell parameters as a result of intercalation. This is the proper way to determine the intercalation voltage and is how all voltage quantities are determined in this work. We contrast these values here with the results for unrelaxed calculations. For the *unrelaxed* value the ions in the two structures were placed on the exact positions of the rocksalt parent lattice and no relaxation was allowed after intercalation. This is to assess the direct effect of changes in the electronic structure for different cation arrangements. The voltage difference between the relaxed $tI16$ and $hR4$ configuration of Li and Co is slightly over half a volt. By comparing with the unrelaxed values it is clear that the difference between the two structures is solely due to relaxation. With no relaxation the voltages of the two structures are practically identical. The compounds with $tI16$ and $hR4$, arrangement have each one internal degree of freedom, apart from the cell parameters a and c. The $hR4$ configuration has the higher intercalation voltage because its symmetry allows for an optimal adjustment of the M-O and Li-O bond lengths in the $LiMO_2$ compound. Figure 4 shows the relation between the oxygen displacements in both structures. In the $hR4$ structure (α-$NaFeO_2$) this degree of freedom reduces or lengthens all M-O bonding simultaneously while changing all Li-O bond lengths in the opposite direction. The metal cations therefore remain in perfect octahedral coordination. In the $tI16$ structure the oxygen octahedra become distorted and cannot satisfy all metal-oxygen bond lengths simultaneously. The α-$NaFeO_2$ structure seems therefore optimal for the perspective of a large intercalation voltage. These results also indicate the importance of working with fully optimized geometries when computing properties of these materials. Virtually all previous calculation on these compounds were performed with methods that are not accurate enough to predict relaxation. They are therefore limited to the study of compounds for which the cell parameters have been characterized experimentally and cannot be used to predict novel compounds. This is no limitation with the pseudopotential method.

TABLE V. Average intercalation voltage calculated for $LiCoO_2$ in $hR4$ and $tI16$ configurations. The *unrelaxed* values are calculated with all ions placed on the sites of an ideal rocksalt lattice.

	$hR4$	$tI16$
Relaxed	3.75	3.26
Unrelaxed	4.22	4.14

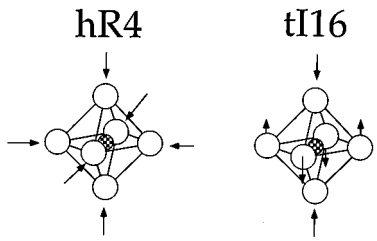

FIG. 4. Effect of the internal relaxation on the metal-oxygen distances in the two structures shown in Fig. 2. In the $hR4$ structure all metal-oxygen and Li-oxygen distances remain equal after relaxation. In the $tI16$ structures the octahedra around the cations become distorted.

V. ELECTRONIC EFFECTS AND BAND STRUCTURE

Most of the compounds used as cathode materials in batteries adapt a structure in which metal cations are coordinated with six anions. Different arrangements of the six anions around the metal can exist. In $LiCoO_2$, Co is octahedrally coordinated, whereas the S ions in $LiMoS_2$ form a trigonal-prismatic arrangement. In the $hR4$ and $tI16$ structures, used in the previous section, all cations are octahedrally coordinated. For a transition metal in octahedral symmetry, the d_{z^2} and $d_{x^2-y^2}$ atomic orbitals directly overlap with the p_x, p_y, and p_z orbitals of the chalcogenide along the octahedral directions. This σ overlap makes up the e_g

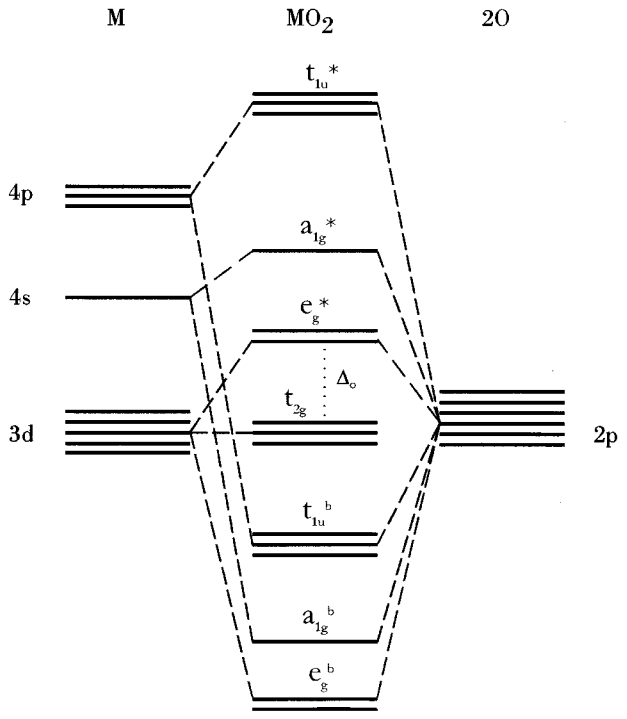

FIG. 5. Schematic of the band structure expected for oxides with octahedrally coordinated transition-metal cations.

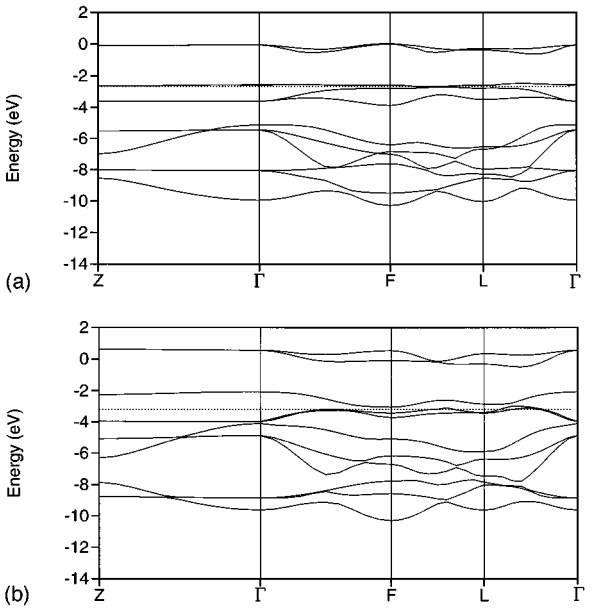

FIG. 6. (a) Partial band structure of $LiMnO_2$. (b) Partial band structure of MnO_2. The dashed line shows the Fermi level.

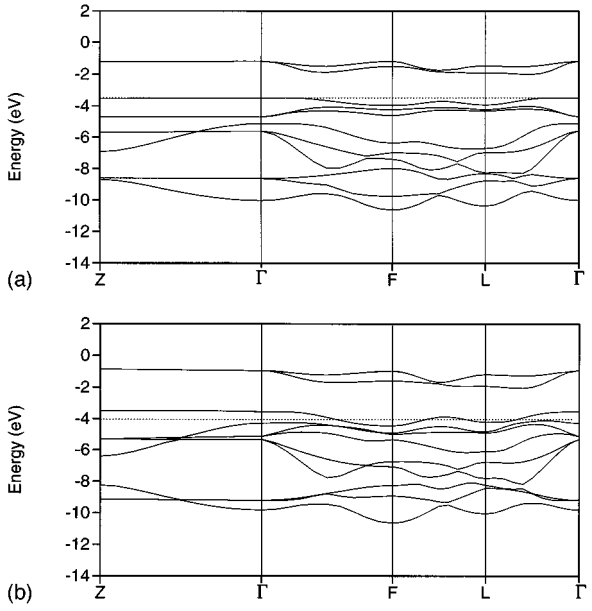

FIG. 7. (a) Partial band structure of $LiCoO_2$. (b) Partial band structure of CoO_2. The dashed line shows the Fermi level.

bands (Fig. 5). For a strongly ionic bond the antibonding band e_g^* mainly consists of the metal d states, whereas the bonding counterpart e_g^b is predominantly of oxygen p character. The remaining d_{xy}, d_{xz}, and d_{yz} orbitals point away from the chalcogenide and have no net σ overlap with its p orbitals (there is some π overlap). These orbitals form a set of nonbonding t_{2g} bands whose width is mainly determined by the metal-metal interaction. In a typical oxide with octahedrally coordinated metals, this mechanism causes the bands to split, as shown in Fig. 5, with the formation of a band gap Δ_O. In addition to the above bands, there are also t_{1u} and a_{1g} bands formed by the overlap of oxygen-p and metal-p, and oxygen-p and metal-s orbitals, respectively. The bonding parts of these bands, shown in Fig. 5, are generally intermixed with each other as well as with the e_g^b band. We shall, from now on, refer to this complex as oxygen bands, since it has mainly an oxygen-p character.

The schematic picture drawn in Fig. 5 for the electronic band structure of octahedrally coordinated solids is clearly identifiable in the true band structure of these materials. For example, in Fig. 6(a), we plotted the pseudopotential band structure for $LiMnO_2$ in the α-$NaFeO_2$ structure along the high-symmetry directions of the rhombohedral Brillouin zone. In this figure the top two bands are the e_g^* bands. They are separated from the three t_{2g} bands by a gap of about 2.5 eV. The six lower bands are the oxygen p bands. This general picture is maintained for all the $LiMO_2$ compounds we have computed although the relative position of the bands shifts with the nature of the metal [compare, for example, the band structure for $LiCoO_2$ in Fig. 7(a)] with that of $LiMnO_2$ in Fig. 6(a), and with the removal of Li [compare Figs. 6(a) and 6(b)].

To investigate the role the metal M plays in the band structure, and the effect of Li intercalation on it, we calculated the density of states of all compounds (Fig. 8). As Li is intercalated into the MO_2 structure, the e_g^* band shifts down and the lower part of oxygen-p band (mainly e_g^b) shifts up. This is consistent with the bond length changes in Fig. 3. Intercalation of lithium increases the M-O bond length leading to a smaller σ overlap between the oxygen-p and metal-d orbitals, thereby pushing the bonding bands up and the antibonding bands down. The level of the t_{2g} band remains almost unchanged (as this is a nonbonding band), but the width of the band changes somewhat. For $M=$Ti the t_{2g} band widens, for V it remains the same, and from Mn to Zn it gets narrower. This observation is a clear effect of the lattice parameter a, which is a direct measure of the M-M distance. For Ti, a decreases with lithiation, for V it is unchanged and from Mn to Zn it increases (see Table II). The upper part of the oxygen-p band, however, is mostly affected by the electrostatics. As we introduce Li^+ between the negatively charged oxygen slabs, the repulsive interaction of these slabs is reduced and the electrostatic energy of the system decreases. This causes the upper part of the oxygen-p band to drop to lower levels.[22] This is clearly seen in the DOS of $LiMO_2$, $M=$Ti–Co. When we change the metal M, from Ti to Zn, the most prominent feature is that bands with mainly metal-d character (t_{2g} and e_g^*) move to a lower energy because of the increase in the nuclear charge of the metal ion.

Several investigators have studied the charge redistribution as a result of Li intercalation. The conventional chemistry picture is to assume that lithium is ionized to Li^+ with the intercalating electron reducing the transition metal from a 4+ to 3+ state. First-principles calculations of the charge transfer have only been applied to $(Li)TiS_2$.[18,19,53] Using the LMTO in the atomic sphere approximation, Guo and Liang found a transfer of only 0.45 electrons per Li atom. However, as they argue themselves, this charge transfer is probably significantly underestimated due to the large sphere size used to count the Li charge. Moreau *et al.*[53] obtains an even smaller charge transfer for the same compound from a Mulliken population analysis in an extended Hückel model. This result is likely due to the somewhat artificial charge assign-

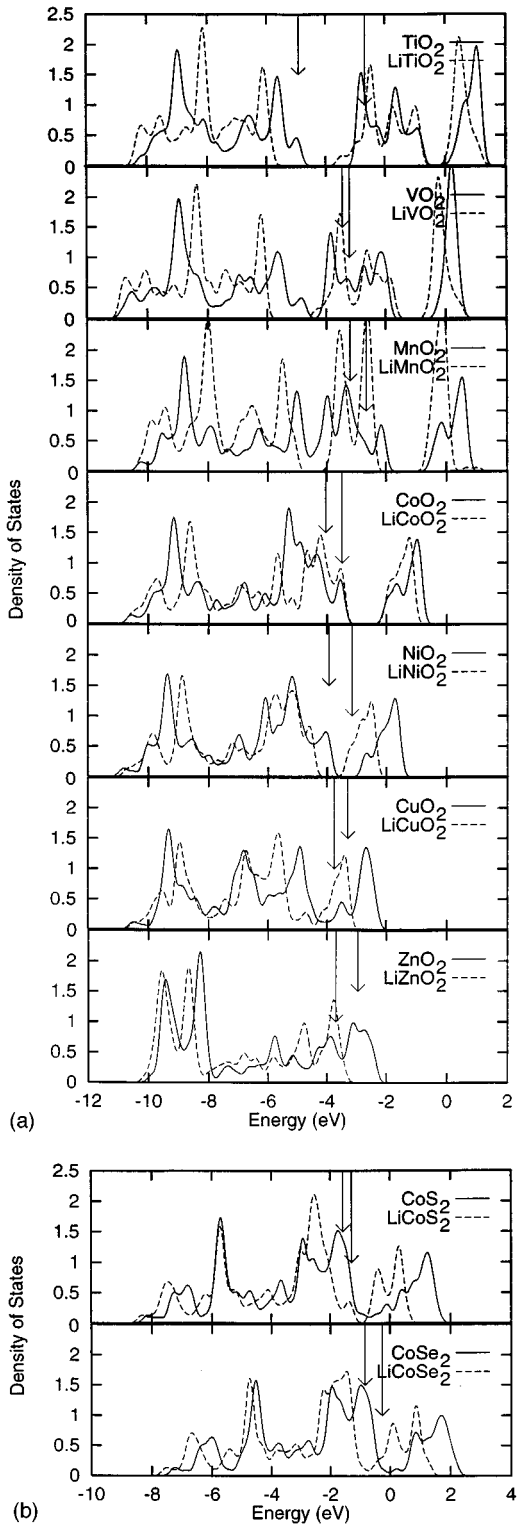

FIG. 8. Density of states for all the LiMX_2 and MX_2 compounds: (a) oxides and (b) sulfides and selenides. The short arrow indicates the Fermi level in MX_2 whereas the long arrow gives the Fermi level in LiMX_2.

ment made in the Mulliken population analysis.

Figure 9 shows the valance electron density of the $LiCoO_2$ in α-$NaFeO_2$ structure. The crystallographic plane shown in this figure is $(11\bar{2}0)$, which is parallel to the c axis. It is clear from the lack of electron intensity at Li sites that Li

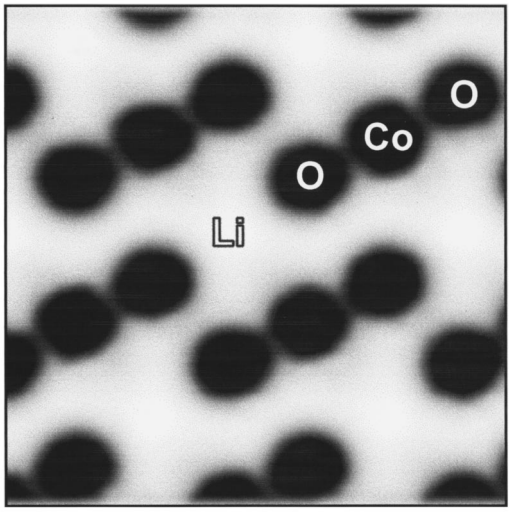

FIG. 9. Valence charge density in layered $LiCoO_2$ in a plane perpendicular to the c axis.

is completely ionized. The layered nature of the structure is also clearly seen. To study the effect of Li intercalation on the electron density, we plot the difference in the electron densities before and after intercalation. For this purpose we calculated both the MO_2 and $LiMO_2$ structures exactly at the same lattice parameters, so that the electron densities can be subtracted point by point in the real space. In Fig. 10 we show the difference in electron density for $LiCoO_2$ in the α-$NaFeO_2$ structure. Only the positive part is shown. Inspection of the negative part (not shown) showed some minor charge depletion around Co. The plane shown is the same as in Fig. 9. As can be observed from the localized electron intensities at oxygen and cobalt ions sites, most of the guest electron is accepted by O and Co. Because the extra charge density around each ion is well localized one can determine the total charge transfer to each ion by integrating the charge density in an appropriate sphere around the ion. Table VI

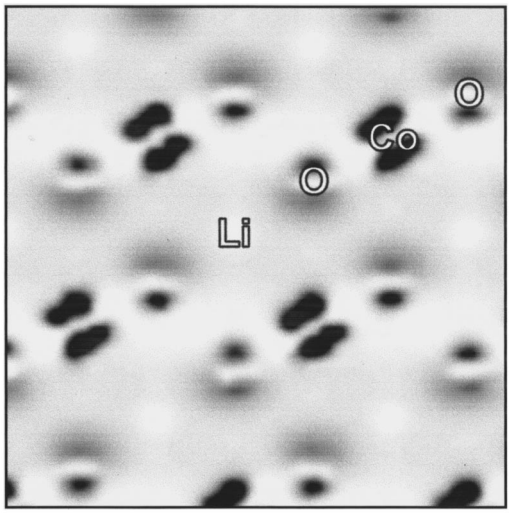

FIG. 10. Positive part of the difference in valence charge between $LiCoO_2$ and CoO_2. Darker shading indicates higher electron density.

TABLE VI. Electron charge-transfer values to X and M upon intercalation of Li into α-$NaFeO_2$ MX_2 structures. The radii of spheres for charge integration are 0.98 and 1.15 Å for M and X, respectively. Note that there are two anions per unit cell.

	Ti-O	V-O	Mn-O	Co-Se	Co-S	Co-O	Ni-O	Cu-O	Zn-O	Al-O
X	0.216	0.245	0.254	0.136	0.152	0.25	0.255	0.261	0.273	0.322
M	0.262	0.253	0.289	0.083	0.135	0.276	0.126	0.102	0.067	0.013

shows the results for the different compounds in the α-$NaFeO_2$ structure. It is interesting to see that the charge transfer to oxygen shows an increasing trend as we go from Ti to Zn and Al. The electron gain of S and Se is very low compared to oxygen. The orbitals involved in this charge transfer can be clearly identified from the charge-difference plots. The shape of the electron clouds localized at the Co site in Fig. 10 has the shape of a d_{xy}-type orbital with the lobes pointing away from the oxygen sites. This is consistent with the filling of the bands. In CoO_2 the electron coming from the intercalated Li ion fills the t_{2g} band [Figs. 7(a) and 7(b)] which is comprised mainly of metal d_{xy}-type orbitals. Figure 11 shows a similar plot for the Ni system. The shape of the intercalating density on the Ni atoms more resembles a d_{z^2} orbital, which is the main component of the e_g^* band.

VI. DISCUSSION

The measured average intercalation voltage in layered $LiCoO_2$ is around 4.0–4.1 V.[54] For $LiVO_2$ in the α-$NaFeO_2$ structure Li intercalation occurs at about 3 V.[55] The voltages predicted in Table III agree fairly well with experimental data although they are consistently lower by about 0.2 V. For the other compounds there is no straightforward comparison with experiments possible. Although on average $LiNiO_2$ has the symmetry of α-$NaFeO_2$, its local symmetry is lower due to a non-co-operative Jahn-Teller distortion (see later).[48] There is also some evidence[43,44] that Ni does not remain in its layer when Li is removed from $LiNiO_2$, but migrates into the Li layer. $LiMnO_2$ usually forms an orthorhombic structure, but has recently[56] been synthesized in a structure that is a monoclinic deformation of α-$NaFeO_2$. The measured average intercalation voltage for that structure was around 3.5 V. Our value of 3.14 V for perfect α-$NaFeO_2$ is somewhat lower which is consistent with the fact that the monoclinic deformation lowers the energy of the compound. It can be shown simply from Eqs. (3) and (4) that all effects that lower the energy of the lithiated compound will increase the average intercalation voltage.

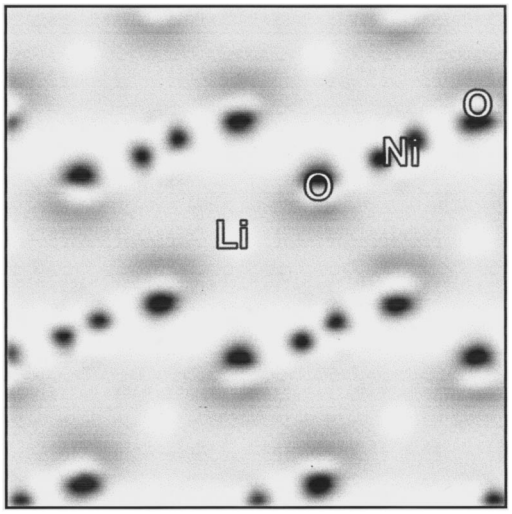

FIG. 11. Positive part of the difference in valence charge between $LiNiO_2$ and NiO_2. Darker shading indicates higher electron density.

To check whether our underprediction of the voltage is due to the pseudopotential approximation or to the local-density approximation, we performed all-electron calculations in the full-potential linear augmented plane-wave (FLAPW) approximation for the voltage in the Co system and found 3.72 V. This value is very close to the pseudopotential result indicating that the pseudopotential approximation does not introduce any significant error. The source of the constant underprediction is likely due to the energy of metallic lithium in Eq. (3). The LDA significantly overpredicts the cohesive energy of Li metal, making it stable by more than 0.4 eV: The experimental value is about 1.6 eV,[57] whereas the LDA gives about 2.0 eV. This overprediction in the binding energy of Li metal will result in a too low voltage. Fortunately, this will result in an identical shift in the voltage for all systems so that the trends deduced from our results should remain valid.

The band structure of the $LiMO_2$ compounds can be explained with ionic molecular-orbital theory: For a compound with an early transition metal such as Ti, the valence bands are mainly of oxygen-p character and are well separated from the metal-derived bands. The latter are almost always split by the octahedral oxygen coordination into three lower t_{2g} and a two upper e_g^* bands. As one goes to the right in the transition-metal series the t_{2g} and e_g^* bands drop in energy and the former mix with the oxygen-p bands.

As M changes from Ti to Co, the M-O bond length decrease in $LiMO_2$, which is likely due to the increasing nuclear charge on the metal, leading to an effectively smaller metal ion. After Co, the bond length increases due to the filling of the antibonding e_g^* bands. For the MO_2 compounds the trend is similar, but the minimum bond length occurs at NiO_2 because these compounds have one electron less than their lithiated equivalents. The filling of the antibonding states therefore only starts at Cu.

Structural effects can be well identified in the band structure. The Li intercalation into the space between the O-M-O slabs pulls the oxygen towards it, effectively increasing the M-O distance (Fig. 3). This reduces the σ overlap of the metal-oxygen bond and causes the lower part of the oxygen-p band to shift upwards by as much as 1 eV. The antibonding counterpart of this band shifts downward by a similar

amount. These shifts in the band structure caused by structural changes clearly limit the application of a rigid-band model.

The effect of structural relaxations on intercalation voltage can clearly be large. The $hR4$ and $tI16$ structure of $LiCoO_2$ differ by 0.5 eV, solely due to relaxation effects. It is therefore unlikely that nonrelaxed calculations can provide any quantitative information. A previous calculation with the X-α method on lithiated and unlithiated clusters fall in this category. Proper relaxation seems difficult to achieve in a cluster calculation because of the artificial boundary conditions. This is not an issue in our calculations as we use periodic boundary conditions on the system. The variation of 0.5 V between two structures is similar to what was found by West *et al.*[58] from comparing the experimentally measured voltages of different Li-V oxides.

Li is clearly fully ionized so that its intercalation effectively donates an electron to the bands of the host material. Our results indicate that the energy level to which this electron is donated is at least qualitatively important for the intercalation voltage. As one goes to the right in the 3-d transition metal series, the metal d states are lower in energy. This is consistent with the increase in intercalation voltage we found. The effect of band structure clearly shows up for the Ni system. The Fermi level for NiO_2 lies in the gap between the filled t_{2g} band and the unfilled e_g^* band. The extra electron in $LiNiO_2$ therefore has to be accommodated in the higher e_g^* band, leading to a significant drop in voltage as compared to the Co compound. After Ni, the voltage again increases as one goes to the later transition metals. The single electron in the narrow e_g^* band causes real $LiNiO_2$ to undergo a Jahn-Teller distortion[48] thereby offsetting at least part of the energy needed to intercalate this electron. Since we did not account for this distortion, the true intercalation voltage for the Ni system will be somewhat higher than what is reported in Table III.

The largest effect on the intercalation voltage comes however from the anion. Substituting S or Se for O significantly reduces the intercalation voltage. This is not surprising if one accepts that a significant part of the electron transfer that accompanies Li is to the chalcogenide, and not to the metal (Fig. 10). The pseudopotential of the chalcogenide therefore contributes to a large extent to the energy level for the intercalating electron. Such a large charge transfer to the anion is not unusual in late transition-metal systems. It has been shown, both theoretically[59] and experimentally[60–62] that acceptor-doped NiO contains oxygen-p rather than metal-d holes. Removal of Li from a material such as $LiNiO_2$ can be seen as another form of hole doping. Charge transfer to the anion was also found by Umrigar *et al.* in their FLAPW calculations on $LiTiS_2$.[18]

One may speculate whether higher intercalation voltages than the 4 V of $LiCoO_2$ are possible. Our results indicate that $LiZnO_2$, if it could be synthesized in the α-$NaFeO_2$ structure would have an average intercalation voltage of 4.4 V (probably more around 4.6, given our consistent underprediction of the voltages by about 0.2 V). This is consistent with our interpretation of the role of the band structure on the intercalation voltage. In $LiZnO_2$ the metal d bands are very low and virtually intermixed with the oxygen-p bands. The electron compensating for the intercalating Li^+ ion can therefore occupy a state with very low energy.

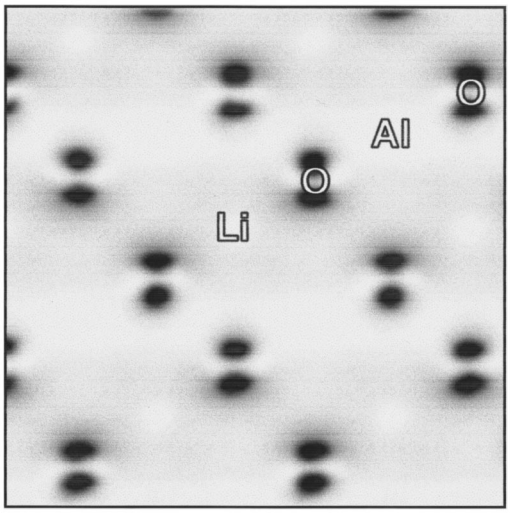

FIG. 12. Positive part of the difference in valence charge between $LiAlO_2$ and AlO_2. Darker shading indicates higher electron density.

Another factor may also be contributing to the higher voltage for the late transition metals. Table VI shows the fraction of the intercalation charge that is transferred to each of the oxygen ions. This value was obtained by integrating the charge in a sphere of radius 1.15 Å around oxygen. The charge transfer to oxygen increases monotonically across the transition-metal series. Shifting the intercalation charge from the transition metal to the oxygen significantly lowers the electrostatic energy of the system as it makes the metal ion more positive and the oxygen ion more negative. In a simple point-charge model the Madelung energy will be approximately proportional to the product of these charges.

Based on this principle, one may ask if there is an upper limit to the Li intercalation voltage in oxides. We have tried to estimate this by intercalating Li in a hypothetical solid O_2 compound (with the same oxygen arrangement as in the α-$NaFeO_2$). The absence of any transition metal leads to a complete transfer of the intercalation charge to the oxygen ions. We calculated that in this material the average intercalation voltage is 5.3 V. This should be compared to the standard oxidation free energy of Li metal with oxygen gas[63] which is -281 kJ per mole of Li, corresponding to 2.91 V. Solid O_2 is of course not very practical as a battery cathode, but the material can be approximated with a compound such as $LiAlO_2$ which is known to exist in the α-$NaFeO_2$ structure. In $LiAlO_2$, the Fermi level lies between the filled oxygen-p band and the unfilled Al sp bands. Removal of Li therefore requires extraction of an electron from the oxygen bands. Charge transfer is therefore completely with oxygen as illustrated by the charge-transfer density in Fig. 12. For intercalation between AlO_2 and $LiAlO_2$ we find an average intercalation voltage of 4.7 only 0.6 V below the intercalation voltage of pure solid O_2.

VII. CONCLUSION

By computing the total energy of a lithiated and the corresponding unlithiated compound, it is possible to predict the

average intercalation voltage for Li. Such an *ab initio* tool should prove to be useful in the design and development of novel cathode materials. The fact that metastable structures may be used for the intercalation compounds in rechargeable batteries—they operate near room temperature—has stimulated a rich field of ''chemistry douce,'' trying to synthesize and test compounds in a large variety of structures. As demonstrated in this paper, first-principles methods can be used to predict the average intercalation voltage in a given structure with fairly high accuracy. This capability can be used to prescreen new compounds before time and resources are put in their synthesis. Although important, voltage is of course not the only selection criterion for Li electrodes.

The capability of predicting intercalation voltages without the need for experimental data also allowed us to systematically investigate the effect of metal, anion, and structure, by computing the intercalation voltage for many hypothetical structures. We find that the anion has a very strong influence on the voltage, with oxygen clearly giving the highest voltages. The important role of the anion can be explained by the significant charge transfer to the anion upon intercalation of lithium. In the oxides, more charge is transferred to the oxygen ions than to the metal ions. Several transition metals (in the α-$NaFeO_2$ structure) give voltages above 3 V, and ZnO_2 and AlO_2 intercalate lithium well above 4 V.

Although the band structure of the materials explains the variation of the voltage with chemistry in a qualitative manner, purely structural effects, such as relaxation, also play a major role, resulting in nonrigid-band intercalation. *Ab initio* methods that do not take into account this relaxation are unlikely to provide quantitative results and will fail to produce most of the band structure changes as a result of Li intercalation.

ACKNOWLEDGMENTS

Support from Furukawa Electric, the Idaho National Engineering Laboratory, and the National Science Foundation under Contract No. DMR-9501856 is gratefully acknowledged. M.K.A. acknowledges partial support from NATO. Supercomputing time was generously provided by the National Science Foundation at the Pittsburgh Supercomputing Center.

[1] *Lithium Batteries*, edited by G. Pistoia (Elsevier, Amsterdam, 1994).
[2] R. B. Goldner, R. L. Chapman, G. Foley, E. L. Goldner, T. Haas, P. Norton, G. Seward, and K. K. Wong, Sol. Energy Mater. **14**, 195 (1986).
[3] R. B. Goldner, F. O. Arntz, G. Berera, T. E. Haas, G. Wei, K. Wong, and P. C. Yu, Solid State Ion. **53-56**, 617 (1992).
[4] J. B. Bates, N. J. Dudney, G. R. Gruzalski, and R. A. Zuhr, J. Power Sources **43**, 103 (1993).
[5] M. B. Armand, J. M. Chabagno, and M. J. Duclot, in *Fast Ion Transport in Solids*, edited by P. Vashista, J. N. Mundy, and G. K. Shenoy (North-Holland, Amsterdam, 1979), p. 131.
[6] J. R. Dahn, A. K. Sleigh, H. Shi, B. M. Way, W. J. Weydanz, J. N. Reimers, Q. Zhong, and U. von Sacken, in *Lithium Batteries*, edited by G. Pistoia (Elsevier, Amsterdam, 1994), pp. 1–49.
[7] K. Mizushima, P. C. Jones, P. J. Wiseman, and J. B. Goodenough, Mater. Res. Bull. **15**, 783 (1980).
[8] T. Nagaura and K. Tozawa, Prog. Batteries Solar Cells **9**, 209 (1990).
[9] L. Heyne, in *Fast Ion Transport in Solids*, edited by W. Van Gool (North-Holland, Amsterdam, 1973), p. 123.
[10] M. S. Whittingham, Prog. Solid State Chem. **12**, 41 (1978).
[11] B. C. H. Steele, in *Fast Ion Transport in Solids*, edited by W. Van Gool (North-Holland, Amsterdam, 1973), p. 103.
[12] P. G. Bruce, A. Lisowska-Oleksiak, M. Y. Saidi, and C. A. Vincent, Solid State Ion. **57**, 353 (1992).
[13] W. Y. Liang, in *Microionics-Solid State Integrable Batteries*, edited by M. Balkanski (North-Holland, Amsterdam, 1991), pp. 237–251.
[14] C. Julien and M. Balkanski, in *Solid State Ionics III*, edited by G. A. Nazri, J. M. Tarascon, and M. Armand, MRS Symposia Proceedings No. 293 (Materials Research Society, Pittsburgh, 1993), pp. 27–37.
[15] J. Friedel, Adv. Phys. **3**, 446 (1954).
[16] D. J. Sellmeyer, in *Solid State Physics: Advances in Research and Applications*, edited by H. Ehrenreich, F. Seitz, and D. Turnbull (Academic, New York, 1978), Vol. 33, p. 83.
[17] J. V. McCanny, J. Phys. C **12**, 3263 (1979).
[18] C. Umrigar, D. E. Ellis, Ding-Sheng Wang, H. Krakauer, and M. Posternak, Phys. Rev. B **26**, 4935 (1982).
[19] G. Y. Guo and W. Y. Liang, J. Phys. C **20**, 4315 (1987).
[20] K. Miura, A. Yamada, and M. Tanaka, Electrochim. Acta **41**, 249 (1995).
[21] J. Rouxel, in *Solid State Ionics*, edited by G. Nazri, R. A. Huggins, and D. F. Shriver, MRS Symposia Proceedings No. 135 (Materials Research Society, Pittsburgh, 1989), pp. 431–442.
[22] W. R. McKinnon, in *Chemical Physics of Intercalation*, edited by A. P. Legrand and S. Flandrois (Plenum, New York, 1987), Vol. B172, pp. 181–194.
[23] A. F. Kohan and G. Ceder, Comput. Mater. Sci. (to be published).
[24] P. Hohenberg and W. Kohn, Phys. Rev. **136**, 864 (1964).
[25] W. Kohn and L. J. Sham, Phys. Rev. A **140**, 1133 (1965).
[26] W. Zhong, D. Vanderbilt, and K. M. Rabe, Phys. Rev. B **52**, 6301 (1995).
[27] M. C. Payne, M. P. Teter, D. C. Allan, T. A. Arias, and J. D. Joannopoulos, Rev. Mod. Phys. **64**, 1045 (1992).
[28] K. M. Glassford and J. R. Chelikowsky, Phys. Rev. B **46**, 1284 (1992).
[29] M. J. Gillan, I. Manassidis, and A. De Vita, Philos. Mag. B **69**, 879 (1994).
[30] Y. Bar-Yam, S. T. Pantelides, and J. D. Joannopoulos, Phys. Rev. B **39**, 3396 (1989).
[31] A. F. Kohan and G. Ceder, Phys. Rev. B **54**, 805 (1996).
[32] K. Kleinman and D. M. Bylander, Phys. Rev. Lett. **4**, 1425 (1982).
[33] A. M. Rappe, K. M. Rabe, E. Kaxiras, and J. D. Joannopoulos, Phys. Rev. B **41**, 1227 (1990).
[34] P. D. Tepesch, G. D. Garbulsky, and G. Ceder, Phys. Rev. Lett. **74**, 2272 (1995).
[35] G. Ceder, Comput. Mater. Sci. **1**, 144 (1993).

[36] D. de Fontaine, in *Solid State Physics: Advances in Research and Applications*, edited by H. Ehrenreich and D. Turnbull (Academic, New York, 1994), Vol. 47, pp. 33–176.
[37] F. Ducastelle, in *Order and Phase Stability in Alloys*, edited by F. R. de Boer and D. G. Pettifor (North-Holland, Amsterdam, 1991), Vol. 3.
[38] J. M. Sanchez, F. Ducastelle, and D. Gratias, Physica A **128**, 334 (1984).
[39] A. Zunger, in *Statistics and Dynamics of Alloy Phase Transformations*, Vol. 319 of *NATO Advanced Study Institute, Series B: Physics*, edited by P. E. A. Turchi and A. Gonis (Plenum, New York, 1994), pp. 361–419.
[40] M. Sluiter, D. de Fontaine, X. Q. Guo, R. Podlovcky, and A. J. Freeman, Phys. Rev. B **42**, 10 460 (1990).
[41] J. N. Reimers and J. R. Dahn, Phys. Rev. B **47**, 2995 (1993).
[42] W. Li, J. N. Reimers, and J. R. Dahn, Phys. Rev. B **46**, 3236 (1992).
[43] J. N. Reimers, W. Li, and J. R. Dahn, Phys. Rev. B **47**, 8486 (1993).
[44] J. Morales, C. Perez-Vicente, and J. L. Tirado, Mater. Res. Bull. **25**, 623 (1990).
[45] K. Mizushuma, P. C. Jones, P. J. Wiseman, and J. B. Goodenough, Solid State Ion. **3/4**, 171 (1981).
[46] M. M. Thackeray, L. A. de Picciotto, W. I. F. David, P. G. Bruce, and J. B. Goodenough, J. Solid State Chem. **67**, 285 (1987).
[47] T. A. Hewston and B. L. Chamberland, J. Phys. Chem. Solids **48**, 97 (1987).
[48] A. Rougier, C. Delmas, and A. V. Chadwick, Solid State Commun. **94**, 123 (1995).
[49] R. J. Cava, D. W. Murphy, S. Zahurak, A. Santoro, and R. S. Roth, J. Solid State Chem. **53**, 64 (1984).
[50] R. Berger and L.-E. Tergenius, J. Alloys Compd. **203**, 203 (1994).
[51] G. G. Amatucci, J. M. Tarascon, and L. C. Klein, J. Electrochem. Soc. **143**, 1114 (1996).
[52] W. B. Pearson, P. Villars, and L. D. Calvert, *Pearson's Handbook of Crystallographic Data for Intermetallic Phases* (American Society for Metals, Metals Park, OH, 1985).
[53] P. Moreau, G. Ouvrard, P. Gressier, P. Ganal, and J. Rouxel, J. Phys. Chem. Solids **57**, 1117 (1996).
[54] T. Ohzuku and A. Ueda, J. Electrochem. Soc. **141**, 2972 (1994).
[55] L. A. De Picciotto, M. M. Thackeray, and G. Pistoia, Solid State Ion. **28–30**, 1364 (1988).
[56] A. R. Armstrong and P. G. Bruce, Nature (London) **381**, 499 (1996).
[57] C. Kittel, *Introduction to Solid State Physics* (Wiley, New York, 1986).
[58] K. West, B. Zachau-Christiansen, T. Jacobsen, and S. Skaarup, in *Solid State Ionics III* (Ref. 14), pp. 39–47.
[59] W. C. Mackrodt, N. M. Harrison, V. R. Saunders, N. L. Allan, and M. D. Towler, Chem. Phys. Lett. **250**, 66 (1996).
[60] P. Kuiper, G. Kruizinga, J. Ghijsen, and G. A. Sawatzky, Phys. Rev. Lett. **62**, 221 (1989).
[61] J. van Elp, H. Eskes, P. Kuiper, and G. A. Sawatzky, Phys. Rev. B **45**, 1612 (1992).
[62] V. R. Galakhov, E. Z. Kurmaev, St. Uhlenbrock, M. Neumann, D. G. Kellerman, and V. Gorshkov, Solid State Commun. **96**, 347 (1995).
[63] *JANAF Thermochemical Tables*, edited by M. Chase (American Institute of Physics for the National Bureau of Standards, Washington, DC, 1985).
[64] T. Ohzuku, A. Ueda, M. Nagayama, Y. Iwakoshi, and H. Komori, Electrochim. Acta **38**, 1159 (1993).
[65] T. Ohzuku, A. Ueda, and M. Kouguchi, J. Electrochem. Soc. **142**, 4033 (1995).